MDPI

Article

Low-Carbon Steel Formed by DRECE Method with Hot-Dip Zinc Galvanizing and Potentiodynamic Polarization Tests to Study Its Corrosion Behavior

Jiřina Vontorová [1],[*] , Vlastimil Novák [1] and Petra Váňová [2]

1 Department of Chemistry and Physico-Chemical Processes, Faculty of Materials Science and Technology, VSB-Technical University of Ostrava, 708 00 Ostrava, Czech Republic; vlastimil.novak@vsb.cz
2 Department of Materials Engineering and Recycling, Faculty of Materials Science and Technology, VSB-Technical University of Ostrava, 708 00 Ostrava, Czech Republic; petra.vanova@vsb.cz
* Correspondence: jirina.vontorova@vsb.cz

Abstract: The use of low-carbon unalloyed steel with minimal silicon content is widespread in structural steel and automotive applications due to its ease of manipulation. The mechanical properties of this steel can be significantly enhanced through severe plastic deformation (SPD) techniques. Our study focuses on the practical benefits of the dual rolling equal channel extrusion (DRECE) method, which strengthens the steel and has implications for material hardness and the thickness of subsequently applied hot-dip zinc galvanizing. Furthermore, the steel's corrosion potential and current are investigated as a function of material hardness and thickness. The findings show a 20% increase in hardness HV 30 after the first run through the forming machine, with an additional 10% increase after the second run. Subsequent galvanizing leads to a further 1–12% increase in HV 30 value. Notably, the DRECE hardening demonstrates no statistically significant effect on the corrosion potential and current; however, the impact of galvanizing is as anticipated.

Keywords: severe plastic deformation; DRECE method; hot dip galvanizing; Zn coating; GDOES; optical microscopy; corrosion; Tafel plot

1. Introduction

DC03 steel is a traditional steel that is appreciated for its ductility characteristics. With its low carbon content, it offers increased elasticity and is easier to shape, bend, weld, and cut. This makes it an ideal option for creating structural components and intricate forms. DC03 steel is commonly utilized in the production of metal furniture, automotive body parts, a variety of industrial components, and electronic equipment.

The DRECE (dual rolling equal channel extrusion) method is part of the SPD (severe plastic deformation) process utilized to enhance the mechanical properties of metals and produce ultrafine-grained (UFG) materials. Through the SPD process, grain sizes of 20 to 200 nm can be achieved [1]. The resulting grain size can be influenced by adjusting the forming parameters (for example, by increasing the deformation pressure or reducing the material temperature during forming) [2]. Additionally, the chemical composition of the material formed significantly influences the resulting grain size [3].

The DRECE forming process involves intensive plastic deformation of the material. The prototype device, located at the Department of Mechanical Technology, Faculty of Mechanical Engineering, VŠB-Technical University of Ostrava, is based on the DCAP method [4–6] (see Figure 1). Figure 1b shows the deformation zone rotated by 180° in the "z" axis (vertical direction) compared to Figure 1a. In 2024, a patent was granted for a new design of a shaping device intended for industrial use.
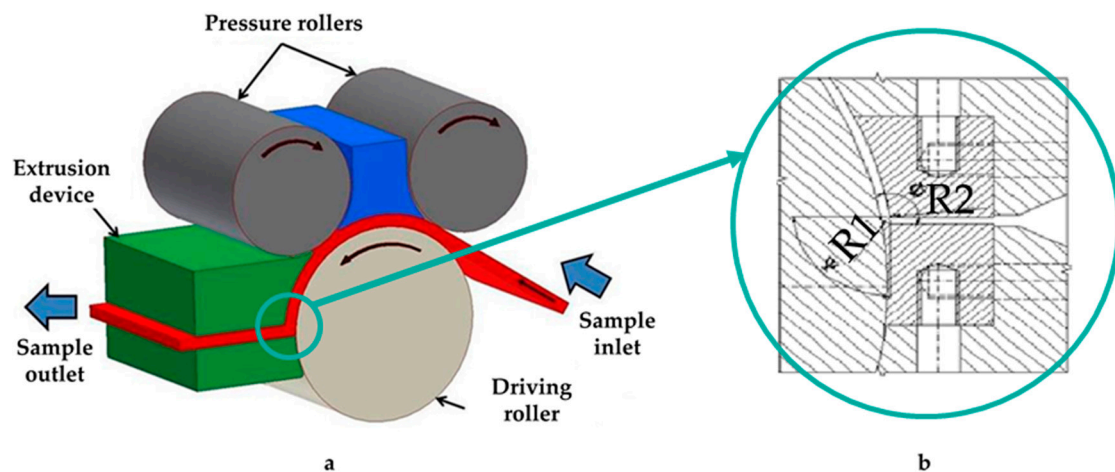
Figure 1. Schematics of the DRECE forming method (adapted from [7]): (**a**) schematics of the equipment and extrusion principle; and (**b**) schematics of the deformation zone.

The main parts of the device are two pressure cylinders, which allow the regulation of the pressure force, and one feed (drive) cylinder. The cylinders are driven by an electric motor with a NORD gearbox via a vane clutch. The belt feed speed range is v = 1–12 mm/s, and the pressure of the rollers can be adjusted in the following range: front roller: p1 = 15–20 MPa, rear roller: p2 = 5–10 MPa, and the motor power input is 0.236 kW.

A piece of sheet metal is fed into the processing area and is pushed through the forming tool by the feed roller, working in tandem with the pressure rollers, without altering the cross-section. The structure can be significantly refined by subjecting the material to multiple plastic deformations in this manner [8]. In reference [7], the authors analyze the impact of severe plastic deformation (SPD) on the quality of DC03 steel at forming tool angles $\Phi = 113°$. The angle at which the forming tool is set in the deformation zone is the most critical factor in determining the efficiency of the forming process, as it enables high deformation intensity and the reshaping of the material [6].

Additional important considerations include the radii R1 and R2 (Figure 1b). Their values are influenced by the characteristics of the strip material. The objective is to achieve shear deformation for grain refinement while ensuring that stress concentrations do not exceed the material's tolerance. In terms of stress distribution, the magnitude of the shear stress must surpass the magnitude of the bending stress during the application of the DRECE method.

In reference [9], the authors describe the effect of increasing the feed rate of the steel strip from 10 mm/s to 100 mm/s, which significantly increased the efficiency of the forming process. Structural analysis on TEM demonstrated a reduction in the mean grain size of the steel strip.

In [10], the authors describe the modernization of the pressing equipment. The deformation zone angle was reduced from 113° to 108°. The mechanical properties after the first pass through the welding machine were increased by 60% for the yield strength Re and by 40% for the ultimate strength Rm. Similar values were also achieved for steel strip DC01 [9].

Hot-dip zinc galvanizing is widely recognized as a highly effective method for safeguarding steel against corrosion [11,12]. This technique facilitates the creation of premium coatings, thereby offering long-term corrosion protection [13] at a reasonable operating cost [14,15]. These coatings serve as a barrier on the steel surface, providing protection against corrosion. Steel corrosion refers to the degradation of metal caused by electrochemical or chemical reactions in a corrosive environment [16].

The process of hot-dip galvanizing steel involves creating an alloy coating of hot-dip zinc on the steel surface. This process involves a series of metallurgical reactions, diffusion, and thermodynamic changes. Standardization for the hot-dip galvanizing of steel parts

can be found in EN ISO 1461 [17] and EN ISO 14713-2 [18]. The quality of the galvanized surface is primarily influenced by the chemical composition. The low silicon content plays a crucial role [19,20], as illustrated by the Sandelin diagram (refer to Figure 2). With regard to the impact of the silicon content on the hot-dip galvanizing process, steels can be categorized based on their silicon content levels as follows [21]: steels with low silicon content (<0.03 wt.% Si); steels falling within the so-called "Sandelin region" with a silicon content in the range of 0.03–0.12 wt.%; steels in the "Sebisty region" with silicon content around (~0.15–0.25 wt.%); and steels with a high silicon content (>0.28 wt.%). Steels with a high silicon content are not recommended for use in the hot-dip galvanizing process due to the resulting thick and brittle coatings, low mechanical resistance, and susceptibility to delamination.
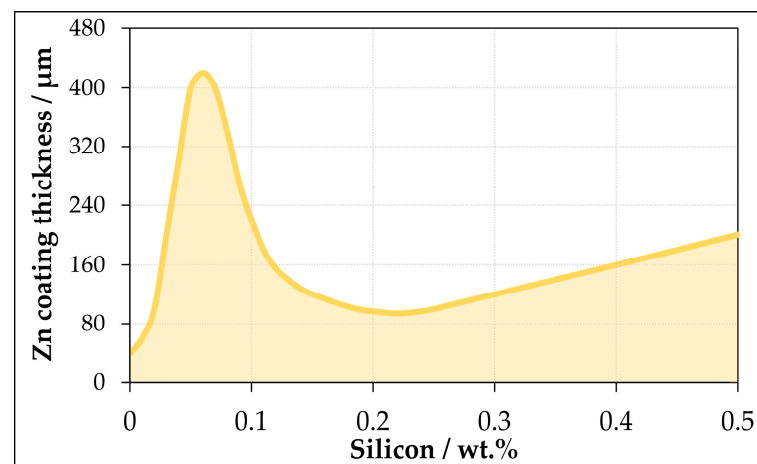
Figure 2. Sandelin diagram.

Depending on the chemical composition of the steel, the temperature of the galvanizing bath, the composition of the bath, the dwell time in the bath, the surface quality and wall thickness of the galvanized material, and the method and rate of cooling, a coating composed of different Fe-Zn intermetallic compounds is formed [22]. These compounds form layers with different grain compositions, morphologies, thicknesses, and mechanical properties [23]. The uppermost layer contains nearly pure zinc, referred to as the η-phase [24]. Beneath this are the monoclinic ζ-phase crystals [25–27], followed by a consistent layer of closely arranged hexagonal δ-phase crystals [27–30]. The bottommost is a thin layer of Γ-phase [31–33].

In the literature [9,10], there is a description of the impact of DRECE forming on the enhancement of steel hardness. However, there is a lack of information regarding the hot-dip galvanizing surface treatment of such a hardened material. This study seeks to address this gap by examining the properties of hardened steel subjected to hot-dip galvanizing.

2. Materials and Methods

For this research, DC03, a low-carbon, low-silicon steel, was selected after applying the DRECE method. The standard for identifying DC03 steel is 1.0347. The low silicon content is crucial for enabling hot-dip galvanizing. The chemical composition of this steel, determined by the BULK GDOES method using a Spectruma Analytik GMBH (Hof, Germany) glow discharge optical emission spectrometer (GDOES) under 700 V and 35 mA excitation conditions [34,35], is presented in Table 1. The elements marked with an asterisk are determined through elemental analysis using an Eltra (Haan, Germany) CS 2000 combustion analyzer [36,37].

Table 1. Chemical composition of DC03 steel.

C*	Mn	Si	P	S*	Cr	Ni	Mo	Cu
				wt%				
0.0406	0.170	0.007	0.013	0.0140	0.028	0.037	0.002	0.061
Ti	**Co**	**B**	**Pb**	**V**	**W**	**Al**	**Nb**	
				wt%				
<0.001	0.006	0.0004	<0.001	0.001	<0.001	0.034	<0.001	

The specimens, which consist of strips of sheet metal measuring 58 mm in width, 2 mm in thickness, and 2000 mm in length, undergo extrusion using the DRECE experimental apparatus (refer to Figure 3). The process parameters are configured at the lower limits of the ranges as mentioned above.
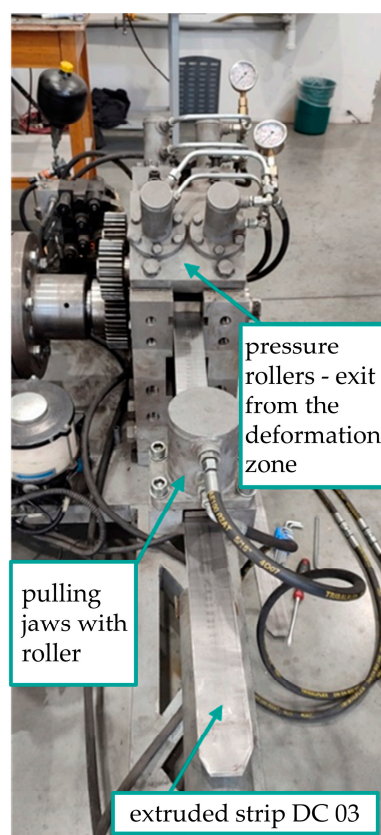
Figure 3. Shaping device. Test progress (photo by author).

The specimens, each approximately 1 m in length, were then subjected to a standard galvanizing process at a hot-dip galvanizing plant. This involves a series of steps, including degreasing, rinsing, pickling with dilute hydrochloric acid, rinsing, immersion in flux, drying, and, finally, immersion in molten zinc, as shown in Figure 4.

Table 2 lists the samples with DRECE and surface treatment. In addition, Figure 5 displays a photograph of the surfaces of all the samples. It is worth noting that the samples without the surface treatment exhibit grooves left by the forming tool, which could potentially impact the mechanical properties of the material being evaluated. Conversely, the galvanizing process results in the formation of a uniform, compact, smooth layer.

Figure 4. Samples after hot-dip galvanizing (photo by author).

Table 2. Description of samples with DRECE and surface treatment.

	Without Surface Treatment		Hot-Dip Galvanized
0	DC03	Z0	DC03
1	DC03, $1\times$ DRECE	Z1	DC03, $1\times$ DRECE
2	DC03, $2\times$ DRECE	Z2	DC03, $2\times$ DRECE
2R	DC03, $2\times$ DRECE with rotation	Z2R	DC03, $2\times$ DRECE with rotation

In the provided description, it can be seen that the microscopic steel images (Figure 6) of samples 0 and 2, denoted as samples in their original state (marked 0) and after two passes through the shaping device (marked 2), with and without the surface treatment (marked Z0 and Z2), correspond to specific structural characteristics. The samples were analyzed in longitudinal and transverse sections, embedded in resin, ground, and polished. The etching was conducted with a Nital 4% reagent. Microstructure observation and zinc layer thickness measurements (see Section 3.1) were performed with an Olympus (Tokyo, Japan) IX70 optical microscope at $200\times$ magnification. The results were analyzed using Image Pro Micro G software (ver. 10).

Upon examination, it was determined that the microstructure of the initial state sample (sample 0) was ferritic, featuring an average grain size of 30 μm, corresponding to a grain size number G = 7 according to standard ISO 643:2021-04 [38]. At this stage, the grains exhibit distinct boundaries. Following zinc galvanizing, the disappearance of certain grain boundaries was noted (sample Z0). A similar microstructure was also observed in sample 2 subsequent to the double passage by the DRECE method. Furthermore, after the zinc galvanizing of the reshaped part, the etchability of the grain boundaries was once again reduced (sample Z2). Notably, the etchability of the microstructure appeared to

deteriorate due to the increased dislocation density and the corrosion protection effect of the zinc coating.

without surface treatment		**hot-dip galvanized**
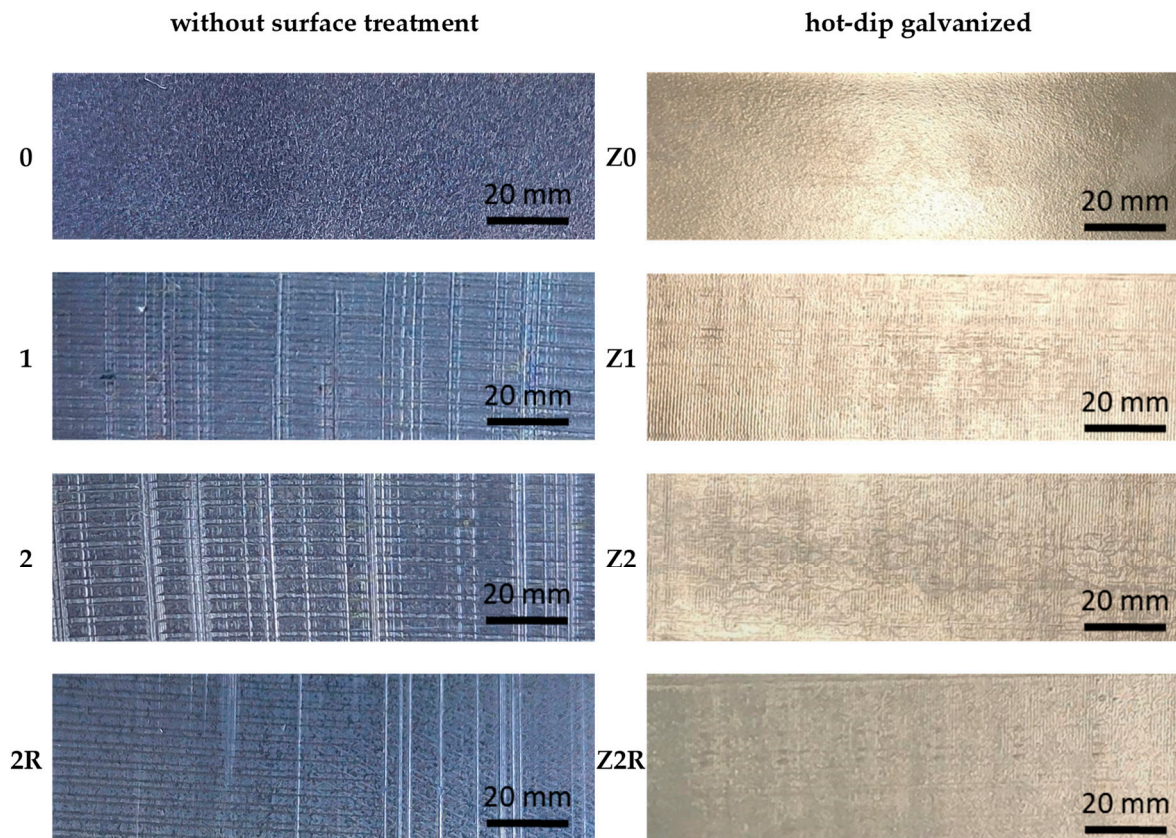
Figure 5. Images of samples under DRECE and surface treatment.

Hardness measurements were performed using the Vickers hardness test according to standard ISO 6507-1:2023 [39]. The measurements were carried out using an EMCO-Test (Kuchl, Austria) DuraScan G5 micro-hardness tester.

The polarization analysis of the steel samples was conducted using the Tafel extrapolation method with a Metrohm Autolab (Utrecht, The Netherlands) PGSTAT302 potentiostat in the standard three-electrode configuration. In this setup, the steel sample functions as the working electrode, an argent chloride (Ag/AgCl) electrode acquired from 2THETA (CR) serves as the reference electrode, and a platinum wire serves as the counter electrode. All experiments were conducted at ambient temperature (25 °C) in 0.1 M HCl, 0.1 M H_2SO_4, and 5% NaCl electrolytes, with chemicals procured from MACH CHEMICALS Ltd. (Ostrava, Czechia); the solutions were diluted using deionized water. The steel samples were immersed in the electrolyte to a depth of 1 cm, and precise adjustment of the immersion was achieved using a micrometer screw. The solutions were purged by nitrogen gas (Messer, Ostrava, Czechia) for 30 min prior to each electrochemical test. The potential was measured at a rate of 2 mV·s^{-1} over a potential range of −1.5 V to 1.0 V. At low polarization rates, the measured currents and voltages convey information about the corrosion process occurring at the interface of the material and electrolyte. In contrast, at high polarization rates, the measured current not only reflects the current value during the corrosion process, but also encompasses the charge of the surface capacitor. Therefore, if the scan rate is not sufficiently low, the current density will exceed that which arises from the corrosion reactions [40]. Although a potential scan rate of 2 mV·s^{-1} was applied, no distortions into the potentiodynamic polarization curves were observed, as has been previously reported [41,42]. No distortions to determine the corrosion current density were observed.

L - direction　　　　　　　　　　　　　　　**T - direction**
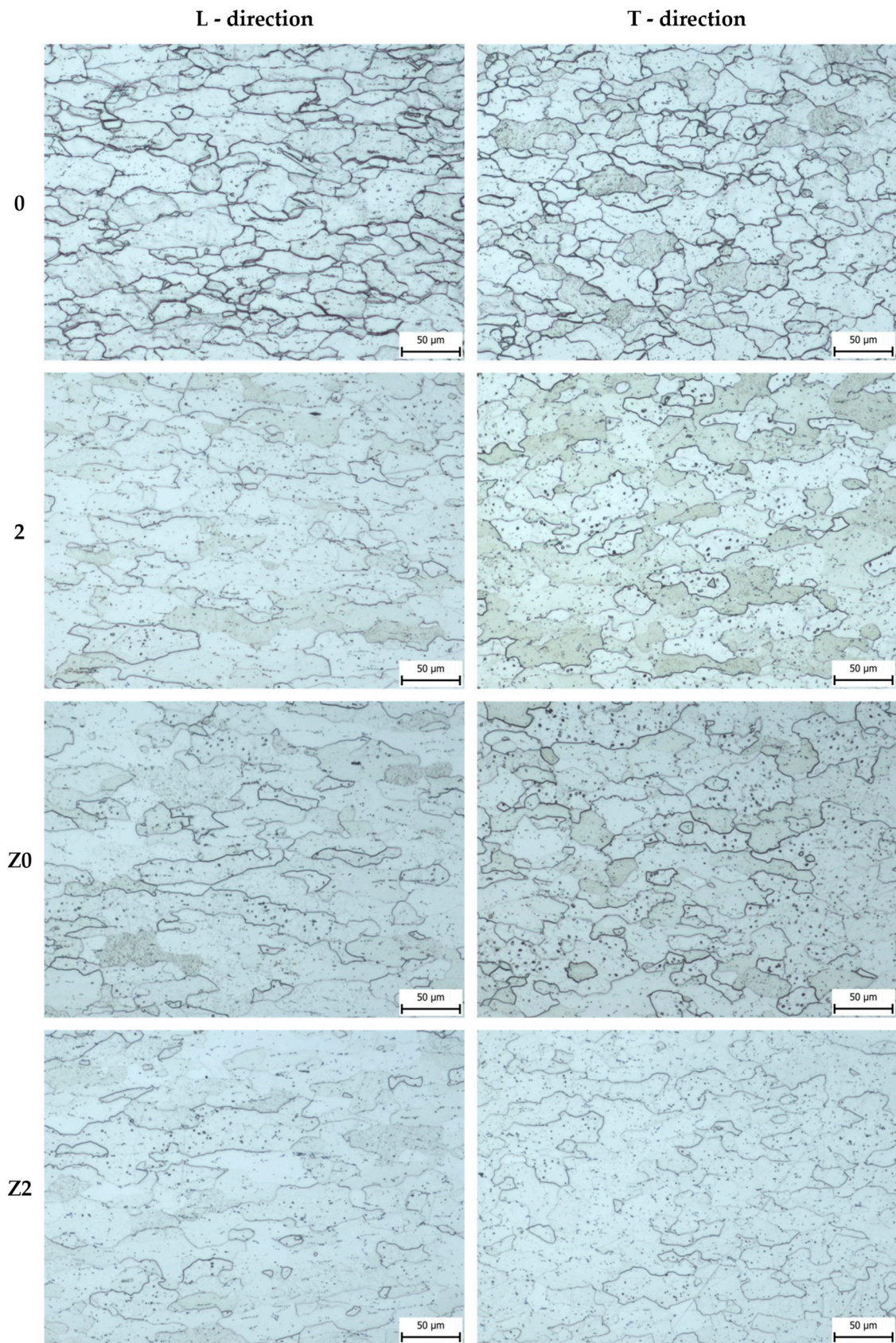
Figure 6. Microscopic images of samples in the longitudinal direction (**L**) and in the transverse direction (**T**).

3. Results and Discussion

3.1. Thickness of the Zinc Layer

The accompanying images display the zinc coating on the base material without DRECE hardening. In Figure 7a, the macroscopic view of the zinc coating on the steel specimen is presented in both the longitudinal (L) and transverse (T) directions. The images depict an impressively even distribution of the zinc coating. Subsequently, Figure 7b illustrates measurements of the zinc coating thickness on samples prepared in both directions.
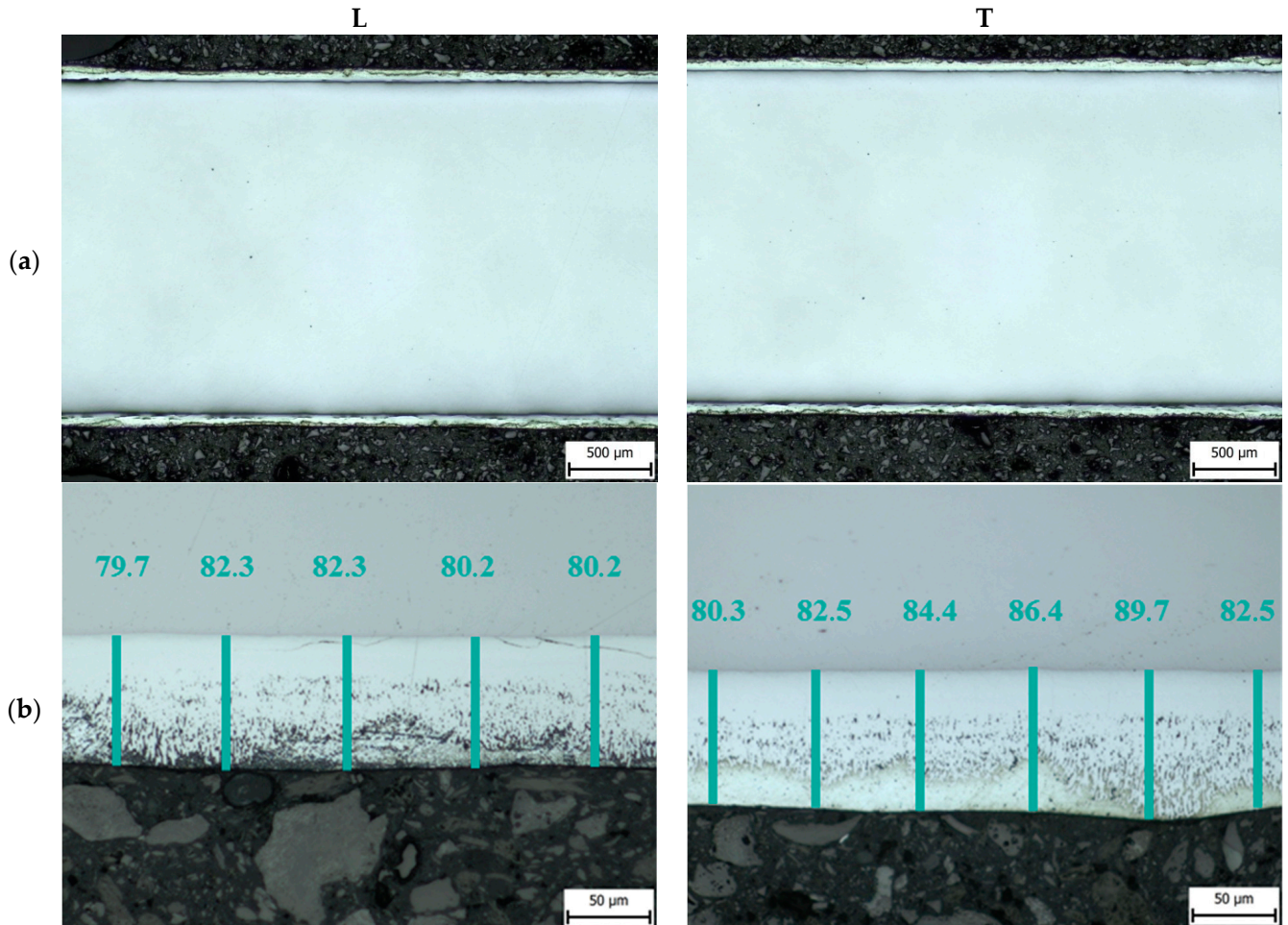
Figure 7. Zn coating on sample Z0 (**a**); and measurement of Zn coating thickness on sample Z0 (**b**). Optical microscopy.

A suitable alternative to optical microscopy for determining the thickness of zinc coatings on planar samples with smooth surfaces is the profile GDOES (Glow Discharge Optical Emission Spectroscopy) analysis. The analysis was performed under the following excitation conditions: 1000 V and 15 mA [43] directly from the surface of the Z0 sample (galvanized sample without DRECE hardening (Figure 8)), 20 mm from the edge of the sample, without sample preparation (cutting, resin potting, polishing, etching). Due to surface heterogeneities, performing GDOES analysis of the galvanized specimens is impossible after DRECE forming.
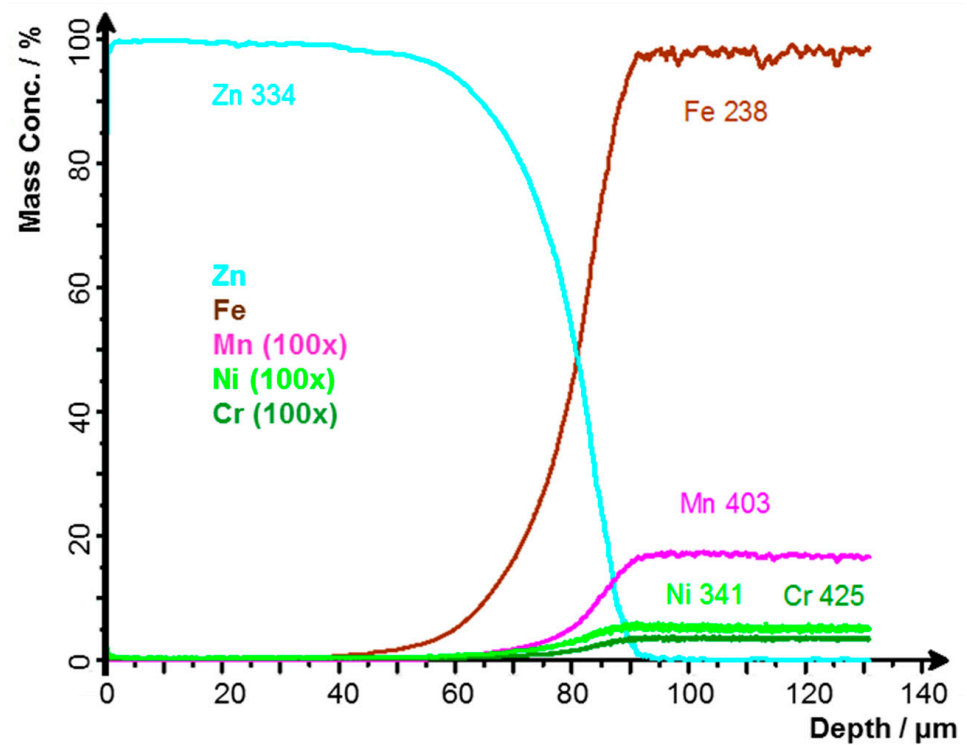
Figure 8. Zn coating thickness measurement on sample Z0, profile GDOES analysis.

The profile curves of zinc and other elements agreed with the results of optical microscopy, revealing a zinc coating thickness of around 80 μm. The measured concentrations also matched those obtained from BULK GDOES analysis (Table 1). It is worth noting that the values extracted from the record must be divided by the number indicated in brackets in the legend of the profile record. The concentrations of certain elements are so low that if the *y*-axis scale remained unchanged, they would be undetectable and indistinguishable from one another.

Figure 9 displays the Zn coating on the steel after DRECE hardening. Additionally, Table 3 illustrates the average layer thicknesses. According to the findings, DRECE hardening results in a minor reduction in the thickness of the subsequent hot-dipped Zn coating. Nevertheless, this reduction is not considered statistically significant.

Table 3. Average thicknesses of Zn coatings/μm.

Sample Label	Thickness of Zn Coating/μm	
	L	T
Z0	80.9 ± 3.1	84.3 ± 3.5
Z1	78.9 ± 3.9	83.6 ± 5.2
Z2	72.5 ± 3.8	71.2 ± 5.3
Z2R	70.7 ± 3.5	75.4 ± 3.8

The coating microstructure corresponds to the requirements for the quality of the hot-dip galvanizing surface treatment. All intermetallic phases, i.e., η, ζ, δ and Γ phases, were identified in the microstructure of the zinc coating. Figure 9b shows the delamination of the zinc coating.
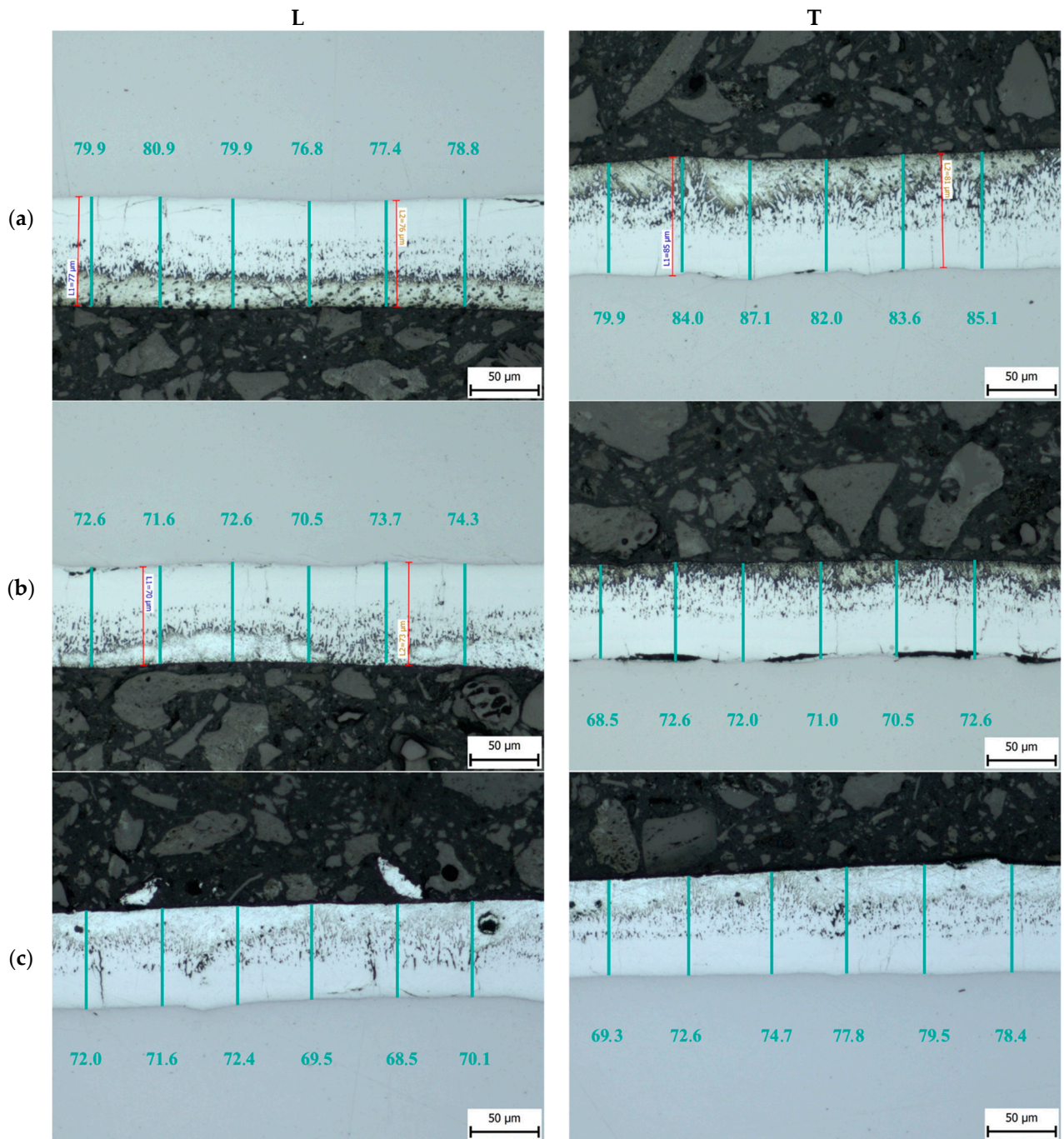
Figure 9. Measurement of Zn coating thickness on sample Z1 (**a**); Z2 (**b**); and Z2R (**c**). Optical microscopy, magnification 200×.

3.2. HV 5 Hardness

The HV 5 hardness of all examined samples was assessed to evaluate the SPD's efficiency. Hardness measurements were made on metallographic sections at the center of the plate thickness. As depicted in Figure 10, the chart illustrates an 18% increase in the base material's hardness after a single pass through the forming machine, followed by an additional 12% increase after a second pass. Subsequent galvanization resulted in a further augmentation of HV 5 by 1–10%.
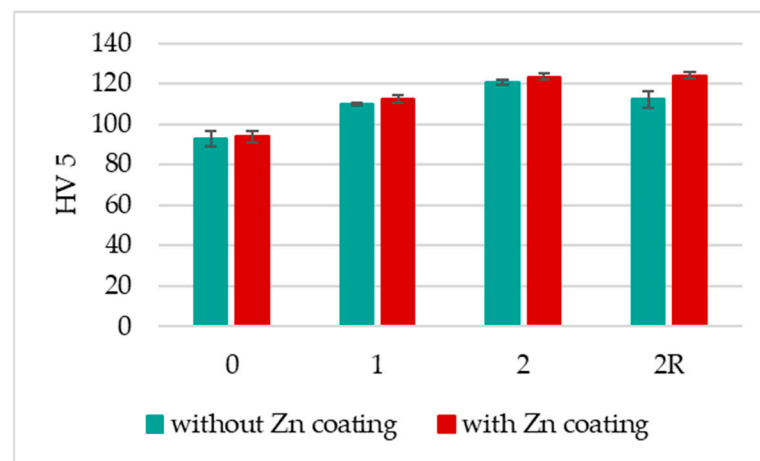
Figure 10. HV 5 hardness of all samples in the L direction.

3.3. Electrochemical Testing

For the electrochemical testing of corrosion behavior, the Tafel extrapolation method is a suitable technique and provides significant time savings compared to the classical immersion method based on mass loss determination. This technique allows for the extrapolation of information relating to corrosion current density (i_{corr}), corrosion potential (E_{corr}), anodic (β_a) and the cathodic (β_c) polarization curve slope and corrosion rate. The measurements are conducted using the linear sweep voltammetry technique, recording current density at varying applied potentials. Subsequently, the recorded data are converted to a logarithm of the current density versus voltage, facilitating the extrapolation process.

In the provided study, Figures 11–13 exhibit the Tafel plots illustrating the behavior of the prepared steel samples in various electrolytes, specifically, 0.1 M HCl, 0.1 M H_2SO_4, and 5% NaCl. In addition, Figure 14 shows repeated measurements of sample 0 in 0.1 M HCl, including Tafel extrapolation. The corrosion potential values for the untreated and DRECE-treated steel samples are relatively consistent, averaging around -0.40 V and -0.41 V when exposed to the corrosive influence of hydrochloric acid and sulfuric acid, respectively. However, a noteworthy shift to -1.07 V was noted for the samples exposed to 5% NaCl. Furthermore, samples subjected to hot-dip galvanizing displayed a noticeable leftward shift in the corrosion potentials compared to the ungalvanized samples, indicating the formation of a protective zinc coating.
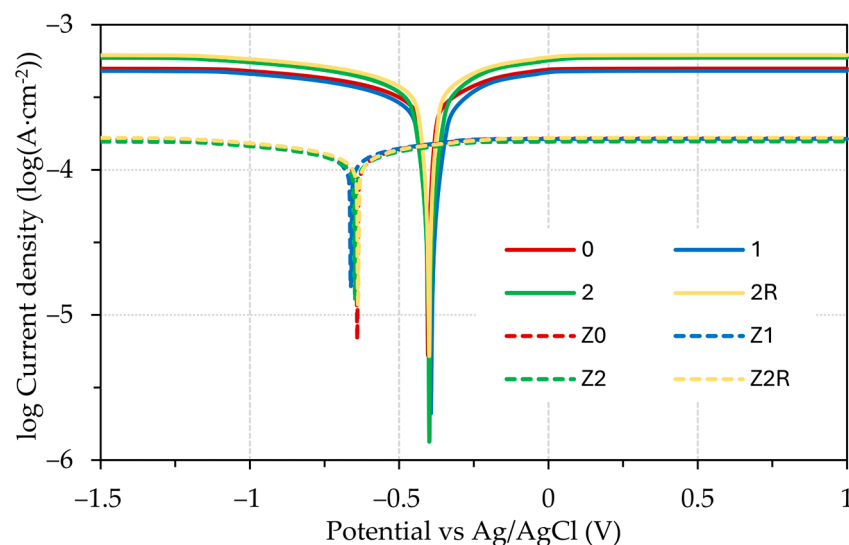
Figure 11. Tafel curves of the tested steel samples in 0.1 M HCl solution.
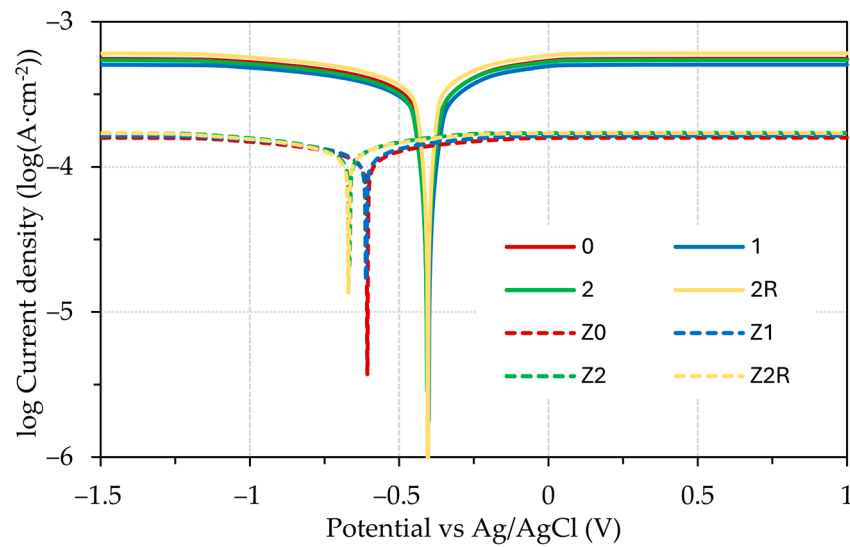
Figure 12. Tafel curves of the tested steel samples in 0.1 M H_2SO_4 solution.
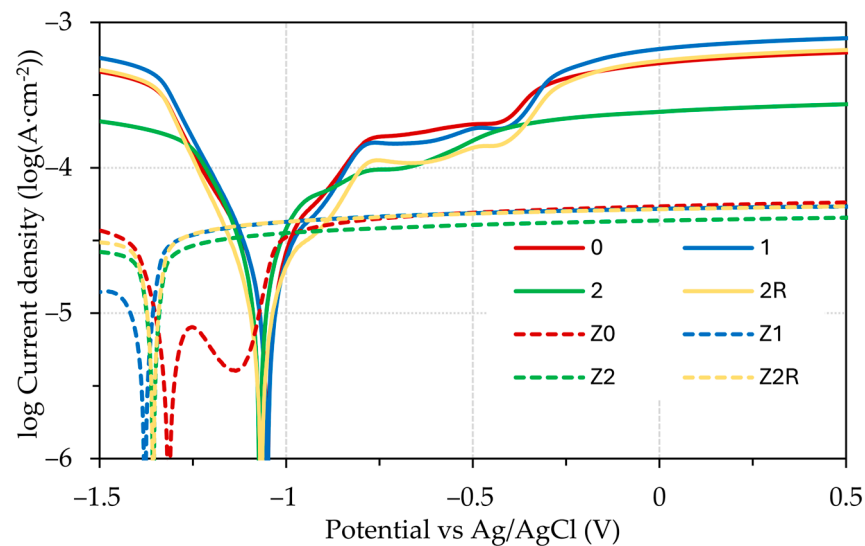
Figure 13. Tafel curves of the tested steel samples in 5% NaCl solution.

Additionally, significant variations in the corrosion current and corrosion rate are observed based on the treatment method and the specific electrolytic medium used. Notably, galvanized steels exhibit markedly lower values for these parameters, underscoring the enhanced corrosion resistance associated with this treatment method.

The data presented in Table 4 illustrate the Tafel extrapolation results for the steel samples tested in three different media. The findings indicate a significant enhancement of corrosion resistance for the hot-dip galvanized steels, as evidenced by the computed corrosion rates. It is noteworthy that the slopes of the anodic polarization curves (β_a) are generally steeper than those of the cathodic polarization curves (β_c), suggesting that the electrochemical polarization of the samples is predominantly governed by anodic processes, with the anodic reaction being more dominant than the cathodic reaction. However, it is important to note that exceptions were observed for samples tested in 5% NaCl. In addition, the polarization resistance values were significantly higher in the samples that underwent hot-dip galvanizing, attributed to the development of a protective layer on the surface. However, it is worth noting that exceptions were observed for samples tested in 5% NaCl.
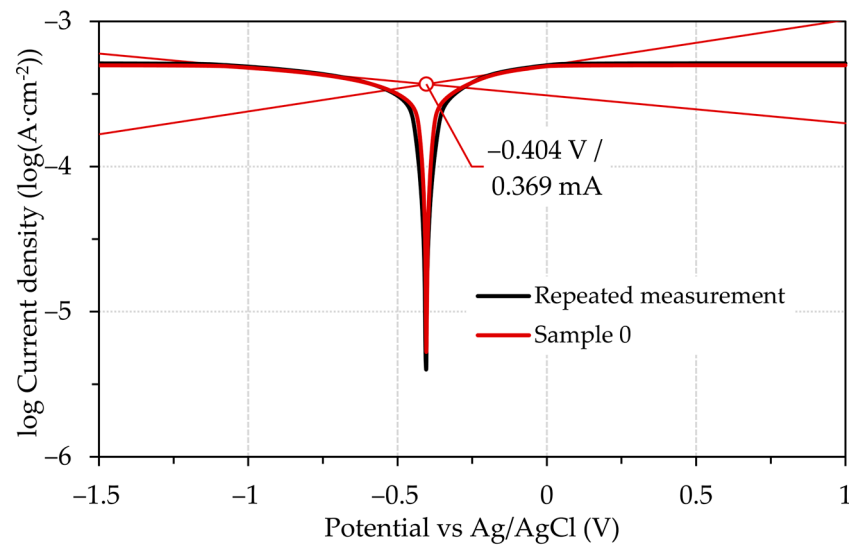
Figure 14. Repeated recording of the polarization potentiodynamic curve of sample 0 in 0.1 M HCl. The original recording shows the Tafel extrapolation.

Table 4. Parameters of Tafel extrapolation for tested samples in different electrolytes.

	0	1	2	2R	Z0	Z1	Z2	Z2R
	0.1 M HCl							
E_{corr} (V)	$-0.404 \pm$ 0.0471	$-0.394 \pm$ 0.0305	$-0.404 \pm$ 0.0316	$-0.404 \pm$ 0.0522	$-0.641 \pm$ 0.0312	$-0.663 \pm$ 0.0311	$-0.649 \pm$ 0.0304	$-0.642 \pm$ 0.0369
i_{corr} (mA·cm^{-2})	$0.369 \pm$ 0.0300	$0.350 \pm$ 0.0315	$0.422 \pm$ 0.0311	$0.447 \pm$ 0.0314	$0.127 \pm$ 0.0374	$0.125 \pm$ 0.0309	$0.122 \pm$ 0.0301	$0.128 \pm$ 0.0319
β_a (V·decade^{-1})	0.315	0.333	0.326	0.315	0.291	0.310	0.277	0.259
β_c (V·decade^{-1})	-0.192	-0.197	-0.196	-0.190	-0.225	-0.248	-0.219	-0.215
Corrosion rate (mm·year^{-1})	4.376	4.143	4.999	5.300	1.504	1.478	1.449	1.515
Polarization resistance (Ω)	2318	2348	1972	1922	6638	6240	7154	7153
	0.1 M H$_2$SO$_4$							
E_{corr} (V)	$-0.409 \pm$ 0.0570	$-0.405 \pm$ 0.0500	$-0.411 \pm$ 0.0420	$-0.409 \pm$ 0.0549	$-0.610 \pm$ 0.0403	$-0.614 \pm$ 0.0523	$-0.675 \pm$ 0.0439	$-0.672 \pm$ 0.0452
i_{corr} (mA·cm^{-2})	$0.403 \pm$ 0.0451	$0.374 \pm$ 0.0410	$0.394 \pm$ 0.0437	$0.441 \pm$ 0.0400	$0.117 \pm$ 0.0461	$0.121 \pm$ 0.0427	$0.132 \pm$ 0.0517	$0.130 \pm$ 0.0423
β_a (V·decade^{-1})	0.316	0.303	0.321	0.308	0.368	0.384	0.296	0.302
β_c (V·decade^{-1})	-0.199	-0.188	-0.193	-0.187	-0.323	-0.317	-0.248	-0.244
Corrosion rate (mm·year^{-1})	4.774	4.437	4.673	5.225	1.384	1.428	1.559	1.539
Polarization resistance (Ω)	2093	2360	2141	1991	5378	5141	6063	6132
	5% NaCl							
E_{corr} (V)	$-1.052 \pm$ 0.0327	$-1.049 \pm$ 0.0310	$-1.070 \pm$ 0.0596	$-1.062 \pm$ 0.0321	$-1.304 \pm$ 0.0524	$-1.364 \pm$ 0.0375	$-1.366 \pm$ 0.0300	$-1.364 \pm$ 0.0356
i_{corr} (mA·cm^{-2})	$0.018 \pm$ 0.0331	$0.017 \pm$ 0.0302	$0.019 \pm$ 0.0422	$0.011 \pm$ 0.0343	$0.004 \pm$ 0.0380	$0.004 \pm$ 0.0302	$0.004 \pm$ 0.0304	$0.004 \pm$ 0.0409
β_a (V·decade^{-1})	3.764	3.674	4.119	4.363	7.535	31.218	14.500	11.622
β_c (V·decade^{-1})	-4.237	-4.862	-4.894	-5.549	-8.728	-6.952	-24.901	-22.506
Corrosion rate (mm·year^{-1})	0.211	0.201	0.230	0.125	0.048	0.049	0.046	0.049
Polarization resistance (Ω)	3044	3004	2488	4170	6602	2737	2850	3085

4. Conclusions

This research delves into the impact of DRECE treatment on the subsequent formation of zinc coating through hot-dip galvanizing. The primary focus was to evaluate the influence of the introduced changes on the resulting corrosion resistance, which was analyzed electrochemically using the Tafel extrapolation method. The findings can be summarized as follows:

- The DRECE method showcases its potential to enhance the hardness of the non-alloy structural steel under examination;

- It is established that applying the DRECE method does not diminish the thickness of the zinc coating of the steel specimens;
- Tafel extrapolation confirmed that the DRECE method has no effect on the corrosion resistance of the tested steel specimens;
- According to Tafel extrapolation, the impact of the DRECE method on corrosion resistance is negligible. Conversely, the hot-dip galvanizing of steel significantly enhances its corrosion resistance, which was demonstrated by a 3–4 fold reduction in the corrosion rate and a drop in the corrosion potential value;
- The influence of the electrolyte used is minimal in the case of the 0.1 M HCl and H_2SO_4 solution. However, when a 5% NaCl solution is employed, the corrosion rate experienced a significant decrease.

The DRECE method is a valuable tool that refines steel by increasing its yield strength and tensile strength in addition to its hardness while reducing its elongation. To the best of our knowledge, the coupling of the DRECE method with hot-dip galvanizing has not yet been published. This combination not only introduces the aforementioned properties but also improves the corrosion resistance of the treated steel. The potential applications of this method are vast, from the construction to the automotive industries, thereby significantly expanding its potential impact.

Author Contributions: Conceptualization, J.V.; methodology, J.V., V.N. and P.V.; validation, J.V., V.N. and P.V.; formal analysis, J.V. and V.N.; investigation, J.V., V.N. and P.V.; resources, J.V., V.N. and P.V.; data curation, J.V., V.N. and P.V.; writing—original draft preparation, J.V., V.N. and P.V.; writing—review and editing, J.V. and V.N. All authors have read and agreed to the published version of the manuscript.

Institutional Review Board Statement: Not applicable.

Informed Consent Statement: Not applicable.

Data Availability Statement: The original data presented in the study are openly available in ZENODO at https://zenodo.org/records/13364426, accessed on 27 August 2024.

Conflicts of Interest: The authors declare no conflicts of interest.

References

1. Toth, L.S.; Gu, C. Ultrafine-Grain Metals by Severe Plastic Deformation. *Mater. Charact.* **2014**, *92*, 1–14. [CrossRef]
2. Valiev, R.Z.; Islamgaliev, R.K.; Alexandrov, I.V. Bulk Nanostructured Materials from Severe Plastic Deformation. *Prog. Mater. Sci.* **2000**, *45*, 103–189. [CrossRef]
3. Zrnik, J.; Dobatkin, S.V.; Mamuzič, I. Processing of Metals by Severe Plastic Deformation (SPD)—Structure and Mechanical Properties Respond. *Metalurgija* **2008**, *47*, 211–216.
4. Rusz, S.; Čízek, L.; Michenka, V.; Dutkiewicz, J.; Salajka, M.; Hilšer, O.; Tylšar, S.; Kedroň, J.; Klos, M. New Type of Device for Achievement of Grain Refinement in Metal Strip. *Arch. Mater. Sci. Eng.* **2014**, *69*, 38–44. [CrossRef]
5. Rusz, S.; Klyszewski, A.; Salajka, M.; Hilser, O.; Cizek, L.; Klos, M. Possibilities of Application Methods DRECE in Forming of Non-Ferrous Metals. *Arch. Metall. Mater.* **2015**, *60*, 3011–3016. [CrossRef]
6. Rusz, S.; Hilser, O.; Ochodek, V.; Cada, R.; Svec, J.; Szkandera, P. Influence of SPD Process on Low-Carbon Steel Mechanical Properties. *MM Sci. J.* **2019**, *2019*, 2910–2914. [CrossRef]
7. Rusz, S.; Kraus, M.; Hilšer, O.; Švec, J.; Kedroň, J.; Čížek, L.; Donič, T.; Tański, T.; Krejčí, L. Increasing the Quality of DC01 Steel by Drece Method. In Proceedings of the METAL 2017-26th International Conference on Metallurgy and Materials, Conference Proceedings, Brno, Czech Republic, 24–26 May 2017.
8. Švec, J.; Rusz, S.; Hilšer, O.; Ochodek, V.; Krejčí, L. Mechanical Properties of Steel DC01 Formed by Drece Method. *Trans. VŠB-Tech. Univ. Ostrav. Mech. Ser.* **2017**, *63*, 63–72. [CrossRef] [PubMed]
9. Jabłońska, M.B.; Kowalczyk, K.; Tkocz, M.; Bulzak, T.; Bednarczyk, I.; Rusz, S. Dual Rolls Equal Channel Extrusion as Unconventional SPD Process of the Ultralow-Carbon Steel: Finite Element Simulation, Experimental Investigations and Microstructural Analysis. *Arch. Civil. Mech. Eng.* **2021**, *21*, 1–11. [CrossRef]

10. Kowalczyk, K.; Jabłońska, M.; Rusz, S.; Bednarczyk, I. Influence of the Drece Process of Severe Plastic Deformation on the Mechanical Properties of the Ultra-Low Carbon Interstitial Free Steel. *Arch. Metall. Mater.* **2018**, *63*, 2095–2100. [CrossRef]

11. Marder, A.R. Metallurgy of Zinc-Coated Steel. *Prog. Mater. Sci.* **2000**, *45*, 191–271. [CrossRef]

12. Kania, H. Structure and Corrosion Resistance of Coatings Obtained by the Batch Double Hot Dip Method in Eutectoid ZnAl Bath with the Addition of Mg and Si. *Coatings* **2022**, *12*, 1207. [CrossRef]

13. Bhat, R.S.; Balakrishna, M.K.; Parthasarathy, P.; Hegde, A.C. Structural Properties of Zn-Fe Alloy Coatings and Their Corrosion Resistance. *Coatings* **2023**, *13*, 772. [CrossRef]

14. Kania, H.; Mendala, J.; Kozuba, J.; Saternus, M. Development of Bath Chemical Composition for Batch Hot-Dip Galvanizing—A Review. *Materials* **2020**, *13*, 4168. [CrossRef]

15. Bellini, C.; Di Cocco, V.; Iacoviello, F.; Mocanu, L.P. Impact of Copper, Tin and Titanium Addition on Bending-Induced Damage of Intermetallic Phases in Hot Dip Galvanizing. *Metals* **2022**, *12*, 2035. [CrossRef]

16. Kreislova, K.; Knotkova, D. The Results of 45 Years of Atmospheric Corrosion Study in the Czech Republic. *Materials* **2017**, *10*, 394. [CrossRef]

17. *EN ISO 1461*; Hot Dip Galvanized Coatings on Fabricated Iron and Steel Articles Specifications and Test Methods. ISO: Geneva, Switzerland, 2022.

18. *ISO 14713-2*; Zinc Coatings—Guidelines and Recommendations for the Protection against Corrosion of Iron and Steel in Structures—Part 2: Hot Dip Galvanizing. ISO: Geneva, Switzerland, 2019.

19. Sánchez, C.; Bustos, O.; Artigas, A.; Bruna, H. Silicon Effect and Microstructural Evolution of Hot Dip Galvanized Coating of Structural Steels. *Metals* **2023**, *13*, 1892. [CrossRef]

20. Vontorová, J.; Mohyla, P. Use of GDOES Method for Evaluation of the Quality and Thickness of Hot Dip Galvanised Coating. *Trans. IMF* **2018**, *96*, 313–318. [CrossRef]

21. Kuklík, V.; Kudláček, J. *Hot-Dip Galvanizing of Steel Structures*; Elsevier, Butterworth-Heinemann: Amsterdam, The Netherlands, 2016; ISBN 9780081007532.

22. Xu, W.; Wang, Y.; Yang, H. Analysis of Measurement Accuracy of Zn–Fe Alloy Coatings under Two Take-off Angles. *Vacuum* **2022**, *205*, 111456. [CrossRef]

23. Vontorová, J.; Mohyla, P.; Kreislová, K. Quality of Zinc Coating Formed on Structural Steel by Hot-Dip Galvanizing after Surface Contamination. *Coatings* **2024**, *14*, 493. [CrossRef]

24. Housecroft, C.E.; Sharpe, A.G. *Inorganic Chemistry*, 4th ed.; Pearson Education Limited: Harlow, UK, 2012; ISBN 978-0-273-74275-3.

25. Gellings, P.J.; Gierman, G.; Koster, D.; Kuit, J. Synthesis and Characterization of Homogeneous Intermetallic Fe-Zn Compounds. *Int. J. Mater. Res.* **1980**, *71*, 70–75. [CrossRef]

26. Belin, R.; Tillard, M.; Monconduit, L. Redetermination of the Iron-Zinc Phase FeZn13. *Acta Crystallogr. C* **2000**, *56*, 267–268. [CrossRef] [PubMed]

27. Okamoto, N.L.; Kashioka, D.; Inomoto, M.; Inui, H.; Takebayashi, H.; Yamaguchi, S. Compression Deformability of Γ and ζ Fe–Zn Intermetallics to Mitigate Detachment of Brittle Intermetallic Coating of Galvannealed Steels. *Scr. Mater.* **2013**, *69*, 307–310. [CrossRef]

28. Okamoto, N.L.; Inomoto, M.; Adachi, H.; Takebayashi, H.; Inui, H. Micropillar Compression Deformation of Single Crystals of the Intermetallic Compound ς-FeZn13. *Acta Mater.* **2014**, *65*, 229–239. [CrossRef]

29. Okamoto, N.L.; Tanaka, K.; Yasuhara, A.; Inui, H. Structure Refinement of the Δ1p Phase in the Fe-Zn System by Single-Crystal X-Ray Diffraction Combined with Scanning Transmission Electron Microscopy. *Acta Crystallogr. B Struct. Sci. Cryst. Eng. Mater.* **2014**, *70*, 275–282. [CrossRef]

30. Okamoto, N.L.; Yasuhara, A.; Inui, H. Order–Disorder Structure of the Δ1k Phase in the Fe–Zn System Determined by Scanning Transmission Electron Microscopy. *Acta Mater.* **2014**, *81*, 345–357. [CrossRef]

31. Hu, X.; Watanabe, T. Relationship between the Crystallographic Structure of Electrodeposited Fe-Zn Alloy Film and Its Thermal Equilibrium Diagram. *Mater. Trans.* **2001**, *42*, 1969–1976. [CrossRef]

32. Yu, J.; Liu, J.; Zhou, W.; Zhang, J.; Wu, J. Cross-Sectional TEM Observation of Iron–Zinc Intermetallic Γ and Γ1 Phases in Commercial Galvannealed IF Steel Sheets. *Mater. Des.* **2007**, *28*, 249–253. [CrossRef]

33. Hu, X.; Zhou, X. Effects of Steel Coatings Microstructure on Weldability in Resistance Spot Welding of Galvannealed Steel Sheets. *Adv. Mater. Res.* **2010**, *139–141*, 610–613. [CrossRef]

34. Weiss, Z. Emission Yields and the Standard Model in Glow Discharge Optical Emission Spectroscopy: Links to the Underlying Physics and Analytical Interpretation of the Experimental Data. *Spectrochim. Acta Part. B At. Spectrosc.* **2006**, *61*, 121–133. [CrossRef]

35. Priamushko, T.S.; Mikhaylov, A.A.; Babikhina, M.N.; Kudiiarov, V.N.; Laptev, R.S. Glow Discharge Optical Emission Spectrometer Calibration Using Hydrogenated Zr-2.5Nb Alloy Standard Samples. *Metals* **2018**, *8*, 372. [CrossRef]

36. Veverka, J.; Vilémová, M.; Chlup, Z.; Hadraba, H.; Lukáč, F.; Csáki, Š.; Matějíček, J.; Vontorová, J.; Chráska, T. Evolution of Carbon and Oxygen Concentration in Tungsten Prepared by Field Assisted Sintering and Its Effect on Ductility. *Int. J. Refract. Met. Hard Mater.* **2021**, *97*, 105499. [CrossRef]

37. Drápala, J.; Brožová, S.; Szurman, I.; Konečná, K.; Kostiuková, G.; Vontorová, J.; Jonšta, P.; Sobotková, K. Influence of Selected Rare Earth Metals on Structural Characteristics of 42CrMo4 Steel. *Metalurgija* **2016**, *55*, 757–760.

38. *ISO 643:2024*; Steels—Micrographic Determination of the Apparent Grain Size. ISO: Geneva, Switzerland, 2024.

39. *ISO 6507-1:2023*; Metallic Materials—Vickers Hardness Test, Part 1: Test Method. ISO: Geneva, Switzerland, 2023; p. 35.

40. Esmailzadeh, S.; Aliofkhazraei, M.; Sarlak, H. Interpretation of Cyclic Potentiodynamic Polarization Test Results for Study of Corrosion Behavior of Metals: A Review. *Prot. Met. Phys. Chem. Surf.* **2018**, *54.*, 976–989. [CrossRef]

41. Zhang, X.L.; Jiang, Z.H.; Yao, Z.P.; Song, Y.; Wu, Z.D. Effects of Scan Rate on the Potentiodynamic Polarization Curve Obtained to Determine the Tafel Slopes and Corrosion Current Density. *Corros. Sci.* **2009**, *51*, 581–587. [CrossRef]

42. Duarte, T.; Meyer, Y.A.; Osório, W.R. The Holes of Zn Phosphate and Hot Dip Galvanizing on Electrochemical Behaviors of Multi-Coatings on Steel Substrates. *Metals* **2022**, *12*, 863. [CrossRef]

43. Vontorová, J.; Váňová, P. Determination of Carburized Layer Thickness by GDOES Method. *AIMS Mater. Sci.* **2018**, *5*, 34–43. [CrossRef]